JOURNAL OF GUIDANCE, CONTROL, AND DYNAMICS
Vol. 26, No. 6, November–December 2003

Normalized Analysis of Interceptor Missiles Using the Four-State Optimal Guidance System

Joel Alpert
Massachusetts Institute of Technology Lincoln Laboratory, Lexington, Massachusetts 02420

Performance prediction of miss distance due to sensor measurement errors and random target manuevers for missiles using proportional navigation guidance has been analyzed using the adjoint technique; a normalization technique has been used to reduce the solution of the set of differential equations describing the proportional navigation guidance problem to a set of algebraic equations using normalized steady-state adjoint miss distance coefficients. The four-state optimal guidance system is generally accepted to yield superior miss distance performance to that of proportional navigation guidance. The previously mentioned normalization technique is described and extended to the four-state optimal guidance system to calculate a new set of values for the normalized steady-state adjoint miss distance coefficients for this configuration. Plots of these normalized coefficients as a function of a normalized tuning parameter provide designers with insight into system performance sensitivities to design parameter and intercept parameter variations. The advantage of this technique is that the results are closed-form equations, and the analyst neither needs to perform simulations nor even to solve the adjoint differential equations. In addition, optimal guidance system results for miss distance due to target spiral maneuver are presented as miss distance normalized to the target maneuver spiral radius, thus providing valuable insights into interceptor performance.

I. Introduction

MISS distance performance due to sensor measurement errors and random target maneuvers of interceptor missiles using proportional navigation guidance has been reduced to a set of algebraic equations and table look-up of normalized steady-state adjoint miss distance coefficients by Zarchan and Nesline using the adjoint technique.[1] These equations have proven to be very useful to missile system analysts and designers. Adjoint analysis[2–8] is an accepted technique of the interceptor missile design community for missile system analysis. It is useful for understanding performance sensitivity to system and intercept parameter variations. These techniques were extended to analysis of command-guided missile systems using synthetic proportional navigation by this author.[9] A more recent paper by Zarchan[10] extends the results to miss distances for missiles using proportional navigation resulting from target weave maneuver.

All of the mentioned equations for the variances of miss distance for each miss distance contributor L can be shown[1] to be a function of power spectral densities ϕ_L of noise sources or random target maneuvers, closing velocity V_C, the sum of the missile time constants τ, and normalized steady-state adjoint miss distance variance coefficient k_L, which is dependent on the distribution of guidance system poles:

$$\sigma^2_{\text{miss}_L} = \phi_L \cdot V_C^{N_L} \cdot \tau^{M_L} \cdot k_L \tag{1}$$

where the exponents N_L and M_L are uniquely defined for each noise or maneuver source of miss distance.

The significance of these algebraic equations is that they can be used to compute quickly expected miss distance components of the total miss distance variances without the use of any simulations; it is simply a matter of assembling the equations, looking up the appropriate steady-state adjoint miss distance variance coefficients k_L, and multiplying by the appropriate intercept parameters:

$$\left(\phi_L \cdot V_C^{N_L} \cdot \tau^{M_L}\right)$$

The total miss distance variance is the sum of the individual miss distance variances calculated for each miss distance contributor L.

A modified form of proportional navigation guidance is the four-state optimal guidance system (OGS).[11] It uses time-varying Kalman filters that are optimized to the time-varying nature of the expected seeker angle measurement noise power spectral density and the expected target maneuver power spectral density. The effective navigation ratio is time varying to compensate for the response time of the autopilot–airframe response (hereafter referred to as the autopilot); the missile acceleration is fed back to the control law. Nesline and Nesline[12] used the adjoint technique for a different analysis of the same optical guidance law coupled with a Kalman filter.

In the OGS problem the normalized steady-state adjoint coefficients are shown herein to be dependent on the expected seeker angle measurement noise power spectral density history normalized

Joel Alpert received B.S. and M.S. degrees in electrical engineering from the University of Wisconsin in 1967 and 1968. Before joining Massachusetts Institute of Technology (MIT) Lincoln Laboratory in 1982, he worked at Raytheon Missile System Division, primarily on missile guidance system design. Earlier Joel Alpert worked at Bell Telephone Laboratories on the Safeguard antiballistic missile system. Since 1982 he has been on the research staff at MIT Lincoln Laboratory in Lexington, Massachusetts, analyzing missile interceptor performance with both analytical and simulation techniques and has done flight testing and data analysis. He is currently working on U.S. Navy ballistic missile defense systems design concepts. He is a Member of AIAA and may be reached at alpert@LL.mit.edu.

Received 28 October 2002; revision received 25 March 2003; accepted for publication 25 April 2003.

to the autopilot time constant (yielding two normalization parameters, T_1 and T_2, which set the normalized spectral noise density history and which are explained in Sec. II), the number and distribution of the autopilot poles, and the number of time constants to go to intercept at which the time-varying navigation ratio is limited (common missile design practice).

In Sec. II the specific mathematical development that leads to the normalization of the OGS problem enabling computation of the steady-state adjoint coefficients is shown; it starts with the OGS block diagram and specification of the expected seeker angle measurement noise power spectral density history. In Sec. III, the normalized steady-state adjoint coefficients of the various miss distance contributors are shown, which provide insight into the performance sensitivities. These normalized steady-state adjoint coefficients are provided so readers may utilize them for their own design and analysis problems. In Sec. IV, two examples of analysis, one for an infrared-guided missile and the other for a radar-guided missile are provided. In Sec. V, concluding remarks and a summary are given. The Appendix contains tables of the coefficient values.

II. Mathematical Development

The continuous four-state OGS block diagram is presented in Fig. 1. and is based on Fig. 6 of Ref. 11, where $N'(T)$ is the time-varying effective navigation ratio and T is time-to-go to intercept, t_{go}, normalized to autopilot time constant τ_{AP}. Notation in this paper is different from that of Ref. 11.

It is has been shown[11] that for the case of time-invariant noise, such as glint, and random maneuver power spectral densities, the steady-state Kalman gains, K_1, K_2, and K_3, are equal to the Weiner filter gains. For slowly time-varying noise power spectral densities with respect to the settling time of the Kalman filter, the Kalman gains, K_1, K_2, and K_3, are approximately equal to the Weiner filter gains; this has been tested in simulation and found to be a very good approximation for typical cases.

The block diagram of Fig. 1 has been manipulated from that of Fig. 6 in Ref. 11 to isolate the Kalman filter from the computation of the zero effort miss (ZEM) and the effective navigation ratio $N'(T)$. The variables n_C and n_A in Fig. 1 are the commanded and achieved missile accelerations by the autopilot, respectively. Figure 1 also contains a target weave (sinusoidal) maneuver, which is not part of the OGS formulation, but is part of the analysis problem to be addressed later in this paper. The maximum weave acceleration is N_W in units of meters per second per second and the weave radian frequency is ω, in radians per second, where $\omega = 2\pi/P_W$, where P_W is the period of the weave in seconds. The block diagram has also been manipulated so that it contains the expression for the radius of the spiral (resulting from a weave in one plane and a weave in the perpendicular plane that is 90 deg out-of-phase with the weave in the first plane), $r_{spiral} = N_W/\omega^2$. The autopilot model is a first-order lag, which is consistent with the assumption used in the development of OGS.

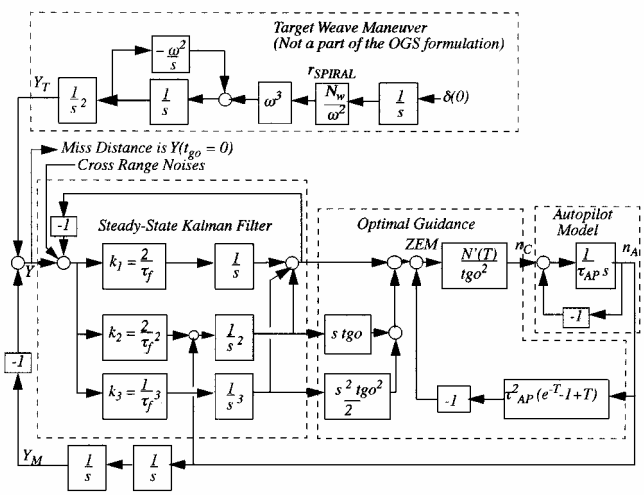

Fig. 1 Block diagram of the four-state OGS and target weave maneuver.

A. Kalman Filter

The Kalman filter, cited in OGS, is represented by its steady-state equivalent, the Weiner filter, which has as its parameter the Kalman filter time constant τ_f, derived from Eq. (8) in Ref. 11:

$$\tau_f = (\phi_N/\phi_M)^{\frac{1}{6}} \tag{2}$$

where ϕ_N is the cross-range measurement noise power spectral density (defined as the seeker angle measurement noise spectral density times missile-to-target range squared).

The design random target maneuver is a step in acceleration, N_T in meters per second per second, whose start time is randomly distributed over a time period of T_M; this random target maneuver is characterized by a power spectral density

$$\phi_M = N_T^2/T_M \tag{3}$$

In Ref. 11, the cross-range noise spectral density is taken to be due only to glint noise, which is independent of range so that the spectral densities and the filter time constant τ_f are time invariant. In the present, more general treatment, the cross-range noise power spectral density is assumed to be time varying as a result of considering the angle noise to be due to range-independent angle noise and active range-dependent angle noise, such as for an active radar seeker (dependent on signal-to-noise ratio), and the change in range and glint; hence, the spectral noise density is given as

$$\phi_N = \phi_{glt} + R^2\left[\phi_{RIN} + \frac{\phi_{RDN_{ref}} R^4}{\left(R_{ref}^4 \sigma_T\right)}\right] \tag{4}$$

where $R = V_C t_{go}$, $\phi_{glt} = \sigma_{glt}^2 \tau_{glt}$, $\phi_{RIN} = \sigma_{RIN}^2/f_s$, and $\phi_{RDN_{ref}}$ is defined as the angle noise spectral density for a 1-m^2 radar cross-section target ($\sigma_T = 1$ m^2) at a range of R_{ref} and, consequently, ϕ_N is time varying; σ_{RIN} is the standard deviation of the range-independent angle noise. The glint correlation time is τ_{glt}, and f_s is the guidance data rate (sampling frequency).

1. *Normalized Kalman Filter*

The normalized Kalman filter is developed next, starting with the normalized steady-state filter time constant. Substituting Eqs. (3) and (4) into Eq. (2) and dividing by the autopilot time constant τ_{AP} yields the normalized Weiner filter time constant $\tau_{fN}(t_{go})$:

$$\tau_{fN}(t_{go}) = \frac{\tau_f(t_{go})}{\tau_{AP}} = \left[\frac{\phi_{glt} + V_C^2 \cdot t_{go}^2 \cdot \phi_{RIN} + V_C^6 \cdot t_{go}^6 \cdot \phi_{RDN_{ref}}/\left(\sigma_T \cdot R_{ref}^4\right)}{\left(\tau_{AP}^6 \cdot N_T^2\right)/T_M}\right]^{\frac{1}{6}} \tag{5}$$

Define t_{go1} to be the time at which the glint noise spectral density equals the range-independent noise spectral density times range squared (Fig. 2),

$$\phi_{glt} = V_C^2 \cdot t_{go1}^2 \cdot \phi_{RIN}$$

then define T_1 to be the normalized time corresponding to t_{go1} measured in units of the autopilot time constant τ_{AP}:

$$T_1 = t_{go1}/\tau_{AP} = 1/(\tau_{AP} \cdot V_C) \cdot (\phi_{glt}/\phi_{RIN})^{\frac{1}{2}} \tag{6}$$

Similarily, at t_{go2} there are T_2 autopilot time constants to go when the range-independent noise spectral density equals the range-dependent noise spectral density:

$$V_C^2 \cdot t_{go2}^2 \cdot \phi_{RIN} = \left(V_C^6 \cdot t_{go2}^6\right) \cdot \phi_{RDN} \tag{7}$$

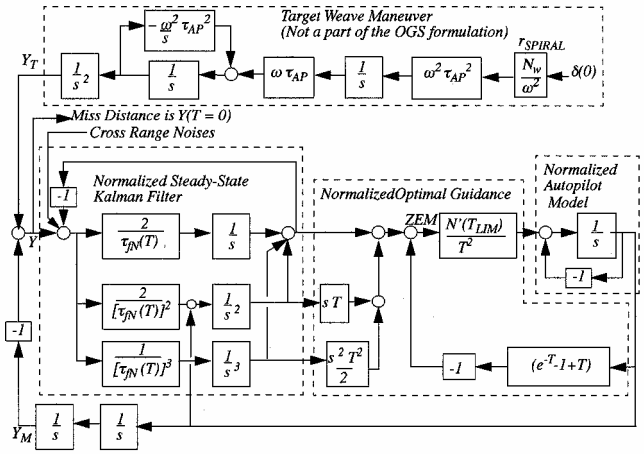

Fig. 2 Block diagram of the normalized four-state OGS and target weave manuever: $T = t_{go}/\tau_{AP}$ and time is in units of τ_{AP}.

where $\phi_{RDN} = \phi_{RDN_{ref}}/(\sigma_T^{\cdot} R_{ref}^4)$. With substitution and manipulation,

$$T_2 = t_{go2}/\tau_{AP} = (1/\tau_{AP} \cdot V_C)(\phi_{RIN}/\phi_{RDN})^{\frac{1}{4}} \tag{8}$$

Hence, the equation for the expected cross-range noise spectral density can be written as

$$\phi_N(T) = V_C^2 \cdot \tau_{AP}^2 \cdot \phi_{RIN} \cdot \left(T_1^2 + T^2 + T^6/T_2^4\right) \tag{9}$$

When it is recalled that range-independent noise power spectral density is

$$\phi_{RIN} = \sigma_{RIN}^2/f_s \tag{10}$$

where σ_{RIN} is the standard deviation of the range-independent angle noise, the normalized Weiner filter time constant in terms of the normalized cross-range noise spectral density parameters can be rewritten as

$$\tau_{fN}(T) = \frac{\tau_f}{\tau_{AP}} = \left[\frac{V_C^2 \cdot T_M \cdot \sigma_{RIN}^2 \cdot \left(T_1^2 + T^2 + T^6/T_2^4\right)}{\tau_{AP}^4 \cdot N_T^2 \cdot f_s}\right]^{\frac{1}{6}} \tag{11}$$

where T_1 and T_2 are given in Eqs. (6) and (8). Note that T_1 and T_2 are not necessarily greater than unity and that T_1 might be larger than T_2.

2. Target Maneuver Spectral Density: A Design Parameter

Theoretically, the values of the maneuver N_T (maneuver acceleration in meters per second per second) and T_M (the period over which the start time of the step target maneuver is uniformly distributed) in the expression for the maneuver spectral density [Eq. (3)] are chosen by the designer to be those of the expected target maneuver. In reality, they are tuning parameters of the design.

Note that in Eq. (11), at one autopilot time constant time to go, $T = 1$, the range-independent noise component of the normalized Weiner filter time constant (given by the T^2 term) has the value given by

$$\Gamma \equiv \left(\frac{V_C^2 \cdot T_M \cdot \sigma_{RIN}^2}{\tau_{AP}^4 \cdot N_T^2 \cdot f_s}\right)^{\frac{1}{6}} \tag{12}$$

which is identified as the normalized tuning parameter and is defined as Γ. Each value of this normalized tuning parameter Γ represents one member of the family of time histories of the normalized Kalman filter time constant during the intercept. Once the tuning parameter Γ is determined along with the values of T_1 and T_2, the normalized system is totally determined, and solutions can be obtained as a function of Γ, T_1, and T_2.

B. Normalization of System Time to Units of Autopilot Time Constant τ_{AP}

This section is presented so that the reader may understand the application of the normalization technique and so that it can be applied to other systems of the reader's choice. The key to the normalization is to convert the OGS system into normalized time, that is, to make the units of time to be τ_{AP} seconds instead of seconds; to accomplish the normalization, the following procedure must be followed so that the numerical values of the output of the integrators remain the same as before the normalization of time (yielding a normalized homing loop):

1) A factor τ_{AP} must be placed in front of each integrator, $(1/s)$, in the block diagram to account for the time change, except for the integrator after the delta function in the target maneuver model because the step function is already in normalized form. Likewise, all factors of s must be divided by τ_{AP}.

2) All expressions of t_{go} must be changed to T by setting $T = t_{go}/\tau_{AP}$ to change time to the normalized time reference.

3) The block diagram must be manipulated by shifting τ_{AP} through blocks of the diagram to cancel all occurrences of τ_{AP} within the homing loop and to move other intercept parameters, V_C, τ_{AP}, N_T, and ϕ, outside the homing loop.

The homing loop consists of the Kalman filter, optimal guidance, autopilot, and the two integrators that yield the missile position Y_M. As a result, a whole set of intercepts can be represented by one normalized adjoint homing loop, and solutions are obtained for all of them with simple multiplication of the appropriate intercept parameters on the outputs of the one normalized adjoint homing loop.

Recall that the time-varying effective navigation ratio for OGS is given by Zarchan and Nesline[11] as

$$N'(T) = \frac{6T^2(e^{-T} - 1 + T)}{2T^3 + 3 + 6T - 6T^2 - 12Te^{-T} - 3e^{-2T}} \tag{13}$$

and note that this is already in normalized form.

The effective navigation ratio, $N'(T)$, which normally increases to very large values at short times to go/τ_{AP}, is limited so that it never gets larger than its value at T_{min}, where T_{lim} is limited time to go normalized to autopilot time constant, $T_{lim} = \text{maximum}(T_{min}, T)$. Because this is a time-varying gain, it is admissible for adjoint analysis. This limiting of the effective navigation ratio also helps the guidance reduce commanded accelerations to keep them below the acceleration capability; this would otherwise occur because the unlimited effective navigation ratio increases to very large values as T approaches zero. Furthermore, this helps prevent possible system instabilities due to errors in time-to-go estimates.

Following the preceding procedure, it is now possible to draw the block diagram of the system of Fig. 1 in normalized form, as Fig. 3, where the normalized Weiner filter time constant $\tau_{fN}(T)$ is given in Eq. (11). Note that the weave maneuver is included in Fig. 3 even though it is not part of the OGS formulation.

C. Normalized Adjoint System

When the rules to construct the adjoint of a block diagram of a linear system[2] are applied, the adjoint of the normalized OGS can be drawn (Fig. 3) with the output being the adjoint impulse response, $h_{glt}(T)$.

In Ref. 9 it is shown that, given the normalized adjoint impulse response of a system $h_{glt}(T)$ (where the impulse response is a function of normalized time T and the integration is also in normalized time), the normalized steady-state adjoint sensitivities, k_0, k_2, k_6, and k_M (representing glint, range-independent noise, active range-dependent noise, and random target maneuver, respectively) can be calculated for each case chosen for specific values of parameters Γ, T_1, T_2, and T_{min}. The steady-state normalized adjoint noise miss distance sensitivities are calculated as

$$k_N = \int_{T=0}^{T=T_{ss}} T^N \cdot h_{glt}^2(T) \cdot dT \tag{14}$$

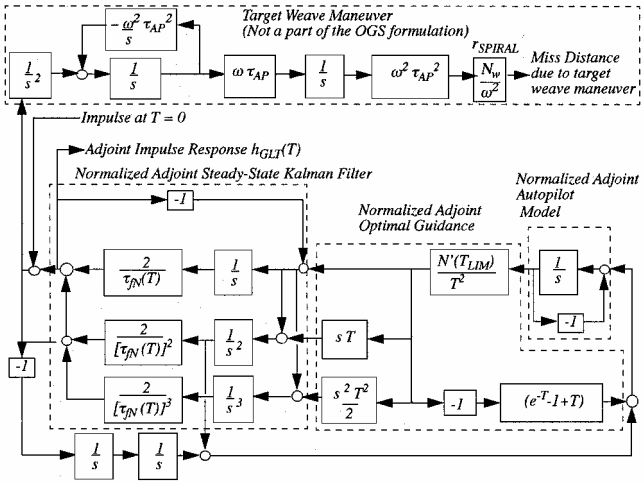

Fig. 3 Block diagram of the adjoint of the normalized four-state OGS and target weave maneuver.

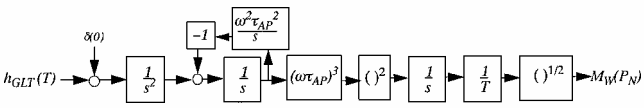

Fig. 4 Block diagram showing computation of normalized weave maneuver miss distance adjoint coefficients.

and the steady-state normalized adjoint uniformly distributed target maneuver miss distance sensitivity is

$$k_M = \int_0^{T_{ss}} \left(\int_0^{T_{ss}} \int_0^{T_{ss}} \left\{ \int_0^{T_{ss}} [h_{glt}(T) + \delta(0)] \cdot dT \right\} \cdot dT \cdot dT \right)^2 \cdot dT \tag{15}$$

where the normalized adjoint impulse response for OGS is a function of the parameters Γ, T_1, T_2, and T_{min} and the normalized time to intercept T: $h_{glt}(T, \Gamma, T_1, T_2, T_{min})$.

It can be shown that the steady-state normalized adjoint maneuver miss distance sensitivity (standard deviation) for weave maneuver can be developed by evaluating the diagram in Fig. 4. Note that the Kalman filter and guidance designs are not optimized to this target weave maneuver.

The statistical miss distances are calculated for each intercept condition using the following algebraic equations:

$$\sigma^2_{miss_{glt}} = k_0(\Gamma, T_1, T_2, T_{min}) \cdot \phi_{glt} \cdot \tau_{AP}^{-1} \tag{16}$$

$$\sigma^2_{miss_{rin}} = k_2(\Gamma, T_1, T_2, T_{min}) \cdot \phi_{rin} \cdot V_C^2 \cdot \tau_{AP} \tag{17}$$

$$\sigma^2_{miss_{rdn}} = k_6(\Gamma, T_1, T_2, T_{min}) \cdot \phi_{rdn} \cdot V_C^6 \cdot \tau_{AP}^5 \tag{18}$$

For a generalized spectral density with a time dependence in cross range of $\phi_N t_{go}^N$,

$$\sigma^2_{miss_N} = k_N(\Gamma, T_1, T_2, T_{min}) \cdot \phi_N \cdot V_C^N \cdot \tau_{AP}^{(N-1)} \tag{19}$$

For a uniformly distributed step maneuver,

$$\sigma^2_{miss_{unifmvr}} = k_M(\Gamma, T_1, T_2, T_{min}) \cdot \phi_{mvr} \cdot \tau_{AP}^5 \tag{20}$$

For weave maneuvers, where $\sigma_{miss_{weave}} = [M_W(P_N\Gamma, T_1, T_2, T_{min})]\tau_{AP}^2 N_W$ and $\omega \cdot \tau_{AP} = 2\pi \cdot \tau_{AP}/P_W = 2\pi/P_N$, where P_N is defined as the normalized weave period, $P_N = P_W/\tau_{AP}$ it follows that

$$\sigma_{miss_{weave}} = [M_W(P_N, \Gamma, T_1, T_2, T_{min})] \cdot N_W / \omega^2 \cdot (2\pi/P_N)^2 \tag{21}$$

Up to this point, all miss distances were for a single plane. The two-plane spiral target manevuer is also of interest, and so the spiral manuever miss distance is $\sqrt{2}$ times the weave miss distance:

$$\sigma_{miss_{spiral}} = M_W(P_N, \Gamma, T_1, T_2, T_{min}) \cdot \sqrt{2} N_W / \omega^2 \cdot (2\pi/P_N)^2 \tag{22}$$

and because the radius of the spiral is

$$r_{spiral} = N_W / \omega^2 \tag{23}$$

then the miss due to a spiral target maneuver can be expressed in terms of the spiral radius as

$$\sigma_{miss_{spiral}} = M_{spiral}(P_N, \Gamma, T_1, T_2, T_{min}) \cdot r_{spiral} \tag{24}$$

where

$$M_{spiral}(P_N, \Gamma, T_1, T_2, T_{min}) = M_W(P_N, \Gamma, T_1, T_2, T_{min}) \cdot \sqrt{2}(2\pi/P_N)^2 \tag{25}$$

III. Normalized Steady-State Adjoint Coefficients

For the case of a single-pole autopilot operating with an infrared (IR) seeker with no glint noise or range-dependent noise ($T_1 = 0$, $T_2 =$ infinity, and $T_{min} = 1$), the numerical values are presented in Table A1 in the Appendix for the single-plane normalized steady-state miss distance variance coefficients for noises and uniformly distributed target maneuver. Table A2 in the Appendix contains the two-plane normalized steady-state miss distance standard deviation coefficients for target spiral maneuver for normalized weave period P_N. Figures 5a and 5b are plots of these variables as a function of the normalized tuning parameter Γ. Even though the spectral density model does not include glint and range-dependent angle noises, the modeled engagement situation might have these noises, and hence, it is of value to have these coefficients, that is, to handle situations where there is a mismatch between the noise model used for the filter design and that of the real world.

Figure 5c is a plot of the same variables as Fig. 5b except that it is presented as curves of different values of the normalized tuning parameter Γ vs normalized weave period, $P_N = P_W/\tau$. Figures 5b and 5c are plots of the miss normalized to the spiral radius so that any miss distance can be calculated by multiplying the normalized miss distance times the radius given by Eq. (23).

In Fig. 5b, miss distances for normalized weave period less than one missile time constant are not plotted because they are all unity, due to the spiral motion being so fast relative to the missile time constant that the missile simply flies up the middle of the spiral, yielding a miss equal to the radius. In Figs. 5b and 5c, note that, for weave periods greater than one missile time constant, the missile has enough time to attempt to follow the maneuver and reduce the miss below the radius value. For large normalized values of normalized tuning parameter Γ, the miss also tends toward unity because the heavier filtering causes the missile to filter out the spiral maneuver and fly up the middle of the spiral.

One can use Fig. 5c to understand the variation in miss distance normalized to spiral radius for a specific target spiral, as a function of autopilot time constant and normalized tuning parameter.

For the case of an autopilot with a single pole operating with an rf seeker with glint noise and no range-independent angle noise ($T_1 = 4$, $T_2 =$ infinity and $T_{min} = 1$), the numerical values are presented in the Appendix in Table A3 for the single-plane normalized steady-state miss distance variance coefficients for noises and uniformly distributed target maneuver and in Table A4 for the two-plane normalized steady-state miss distance standard deviation coefficients for target spiral maneuver normalized for weave period P_N. Figures 6a–6c are equivalent for this case to the plots in Figs. 5a–5c. Note that the spiral miss distances for Figs. 6b and 6c are larger than those for Figs. 5b and 5c because the glint spectral density prevents reduced filtering close to intercept, which causes the maneuver miss to increase. When Fig. 6a is compared to 5a, it is seen that all the miss distance sensitivities increase except for those due to glint noise.

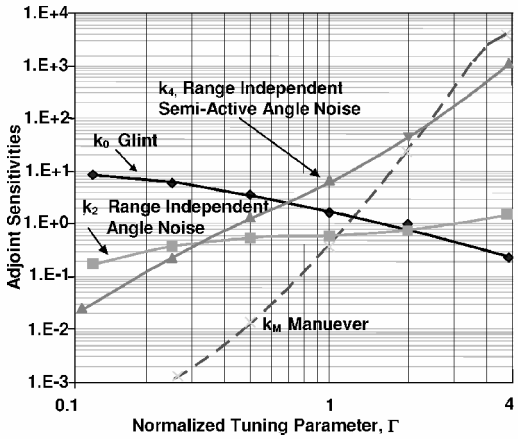

Fig. 5a Single-plane normalized steady-state adjoint coefficients for noise and uniformly distributed target maneuvers vs tuning parameter Γ single-pole autopilot, $T_1 = 0$, $T_2 = \infty$, and $T_{\min} = 1$.

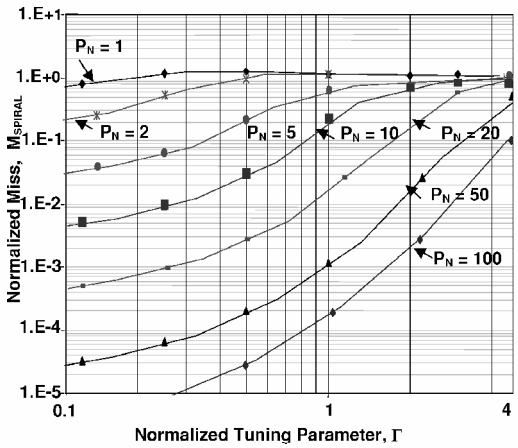

Fig. 5b Two-plane normalized steady-state miss distance for target weave maneuver vs normalized tuning parameter Γ M_{spiral} vs Γ for single-pole autopilot, $T_1 = 0$, $T_2 = \infty$, and $T_{\min} = 1$.

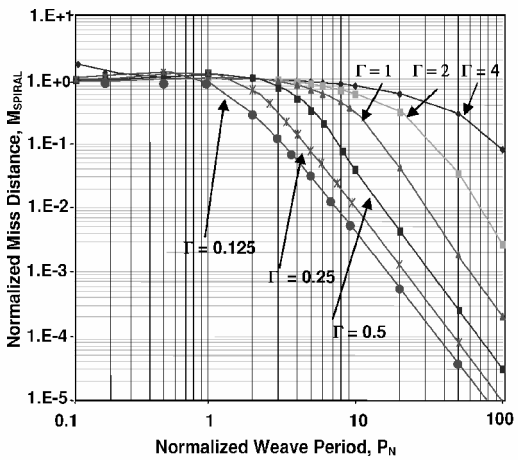

Fig. 5c Two-plane normalized steady-state miss distance for target weave maneuver vs normalized weave period, P_N M_{spiral} vs P_N single-pole autopilot, $T_1 = 0$, $T_2 = \infty$, and $T_{\min} = 1$.

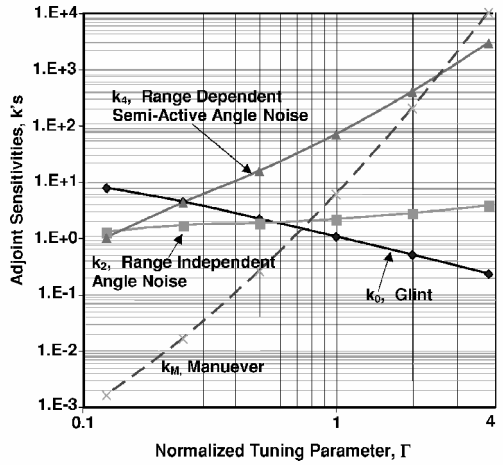

Fig. 6a Single-plane normalized steady-state adjoint coefficients for noise and uniformly distributed target maneuvers vs tuning parameter Γ single-pole autopilot, $T_1 = 4$, $T_2 = \infty$, and $T_{\min} = 1$.

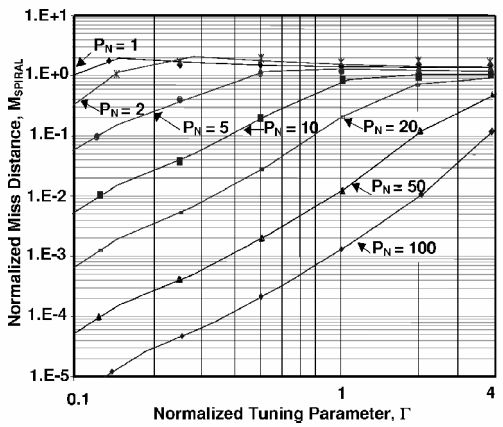

Fig. 6b Two-plane normalized steady-state miss distance for target weave maneuver vs normalized tuning parameter Γ M_{spiral} vs Γ for single-pole autopilot, $T_1 = 4$, $T_2 = \infty$, and $T_{\min} = 1$.

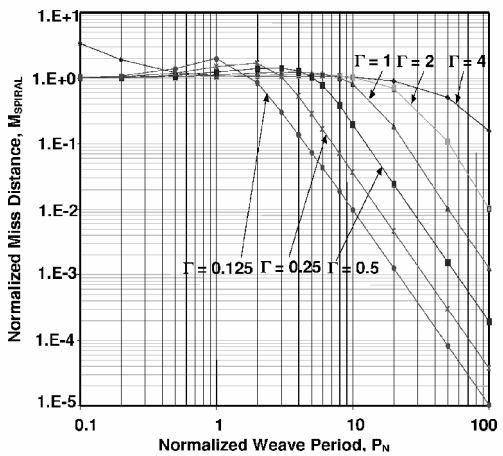

Fig. 6c Two-plane normalized steady-state miss distance for target weave maneuver vs normalized weave period, P_N M_{spiral} vs P_N single-pole autopilot, $T_1 = 4$, $T_2 = \infty$, and $T_{\min} = 1$.

To validate the methodology presented, a set of simulation runs was made for the case of no glint noise given in Table A2. A Monte Carlo simulation representing the forward system given in Fig. 1 with the $N'(T)$ limitation was run, varying the phase of the maneuver with respect to the intercept time, to be equivalent cases to the adjoint results. Four cases were run for the normalized tuning parameter $\Gamma = 1$, over normalized weave periods P_N of 0.1, 1, 5, and 10; for 100 Monte Carlo samples, the results differed from the adjoint results by −0.3, −1.8, −1.7, and −1%, respectively. The parameters used were autopilot time constant τ_{AP} of 0.5 s, time of flight of 100 s, target maneuver acceleration level of 49 m/s/s. The results for the adjoint were obtained by running the adjoint system for 100 s and then computing the root mean square of the results for the last 50 s; this procedure was followed to allow the transients to die out so that it could represent the results for a uniformly distributed probability of phase of maneuver with respect to intercept.

IV. Analysis Examples

In this section the performance of two different seekers for the same intercept conditions is analyzed using the technique discussed in Secs. II and III.

A. Example 1: RF Seeker

In this section a numerical example is presented that illustrates the utility of the normalization method. The parameters of the intercept are $\tau_{AP} = 0.25$ s, missile autopilot time constant; $V_C = 2000$ m/s, closing velocity; $f_s = 50$ Hz, guidance data rate; $\sigma_{RIN} = 0.004$ rad, standard deviation of range-independent angle noise; $\sigma_{glt} = 4$ m, standard deviation of target glint noise; $\tau_{glt} = 0.08$ s, correlation time of target glint noise; $P_W = 5$ s, target weave period; and $N_W = 20$ m/s/s, target weave acceleration.

Therefore, the radius (in meters) of the two-dimensional spiral is

$$r_{spiral} = N_w \big/ \omega^2 = N_w (P_w/2\pi)^2 = 20(5/2\pi)^2 = 12.7$$

Normalized tuning parameter is chosen, $\Gamma = 1$. First the value of T_1 is calculated,

$$T_1 = (1/\tau_{AP} V_C)(\sigma_{glt}/\sigma_{RIN})(\tau_{glt} \cdot f_s)^{\frac{1}{2}}$$

$$= (1/0.25 \cdot 2000)(4/0.004)(0.08 \cdot 50)^{\frac{1}{2}} = 4$$

the normalized time at which glint equals range-independent cross-range spectral density.

The normalized weave period is $P_N = P_W/\tau_{AP} = 5/0.25 = 20$. The procedure for calculating the expected miss distance is to use Tables A3 and A4 in the Appendix and Figs. 6a–6c for the appropriate autopilot configuration, look up the steady-state adjoint miss distance sensitivities, k_0, k_2, k_6, and k_M, and if there is a weave maneuver, calculate $P_N = P_W/\tau_{AP}$, and look up $M_{spiral}(P_N)$ and multiply by the appropriate parameters. In this example, Tables A3 and A4 values were used (single-pole autopilot, $T_1 = 4$, and $T_2 =$ infinity) for tuning $\Gamma = 1.0$.

The following equations can then be evaluated for the single-plane range-independent noise, glint noise, and maneuver miss distances:

$$\sigma^2_{miss_{glt}} = k_0(\Gamma, T_1, T_2, T_{min}) \cdot \phi_{glt} \cdot \tau_{AP}^{-1}$$

$$\sigma_{miss_{glt}} = \sqrt{1.05 \cdot (4^2 \cdot 0.08) \cdot 0.25^{-1}} = 2.3\,\text{m}$$

$$\sigma^2_{miss_{RIN}} = k_2(\Gamma, T_1, T_2, T_{min}) \cdot \phi_{RIN} \cdot V_C^2 \cdot \tau_{AP}$$

$$\sigma_{miss_{RIN}} = \sqrt{2.11\left(\frac{0.004^2}{50}\right) \cdot 2000^2 \cdot 0.25} = 0.8\,\text{m}$$

For weave maneuvers, the single-plane noises are calculated as

$$\sigma_{miss_{weave}} = M_{spiral}(P_w/\tau_{AP}, \Gamma, T_1, T_2, T_{min}) \cdot r_{spiral} \big/ \left(\sqrt{2}\right)$$

$$\sigma_{miss_{weave}} = (0.183 \cdot 12.7) \big/ \left(\sqrt{2}\right) = 1.6\,\text{m}$$

These points are shown in Fig. 7 at the abscissa value of $\Gamma = 1$. Figure 7 also shows the variation of the miss distance as a function of the normalized tuning parameter. Note that, as the normalized tuning parameter is increased, the glint miss decreases, but the range-independent noise and weave maneuver misses increase. The total miss distance, which is the root mean square of the components, reaches its minimum at a value of $\Gamma = 0.8$ for the normalized tuning parameter.

B. Example 2: IR Seeker

For the IR seeker the following parameters differ from those of the RF seeker example: $\sigma_{RIN} = 0.0005$ rad, standard deviation of range-independent angle noise, and $\sigma_{glt} = 0.0$ m, standard deviation of target glint noise (no glint noise). Assume a tuning of $\Gamma = 1.0$. Calculating the normalized parameters for this engagement yields $T_1 = 0$, no glint, and $P_N = P_W/\tau_{AP} = 5/0.25 = 20$ is the normalized weave period.

Use the procedure for calculating the expected miss distance presented in the preceding example, but use Tables A1 and A2 and Figs. 5a–5c for the appropriate parameter values; look up the steady-state adjoint miss distance sensitivities, k_0, k_2, k_6, and k_M, and if there is a weave maneuver, calculate P_W/τ_{AP}, and look up $M_{spiral}(P_N)$. Tables A1 and A2 values were used (single-pole autopilot, $T_1 = 0$, and $T_2 =$ infinity) for tuning $\Gamma = 1.0$:

$$\sigma_{miss_{RIN}} = \sqrt{0.6\left(\frac{0.0005^2}{50}\right) \cdot 2000^2 \cdot 0.25} = 0.06\,\text{m}$$

$$\sigma_{miss_{weave}} = \frac{(0.037 \cdot 12.7)}{\left(\sqrt{2}\right)} = 0.3\,\text{m}$$

Figure 8 shows that the miss distances for the IR seeker case are significantly smaller than those for the rf seeker case because range-independent noises are smaller and there is no glint noise. The normalized miss distance coefficients are lower for the IR case than the rf case, resulting in a reduced miss distance for the weave target maneuver by a factor of five. Even though the range-independent noise is lower by a factor of 8, the miss due to this source is lower by a factor of 15, due to the reduced filtering. In addition, the lower noise levels could allow a smaller value of normalized tuning that reduces the miss distance for the target weave maneuver even further. The choice for best value of the normalized tuning parameter would be limited by issues not

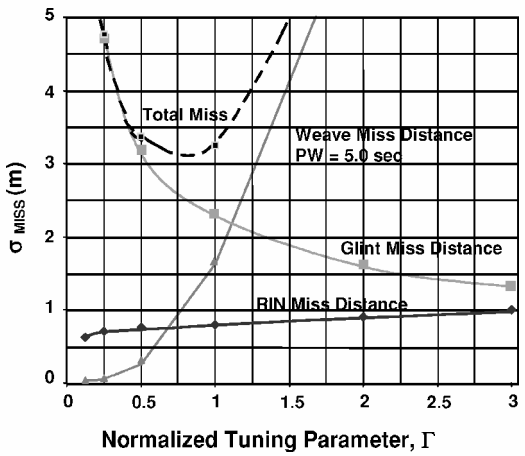

Fig. 7 Miss distance components and total for rf design example vs normalized tuning parameter Γ.

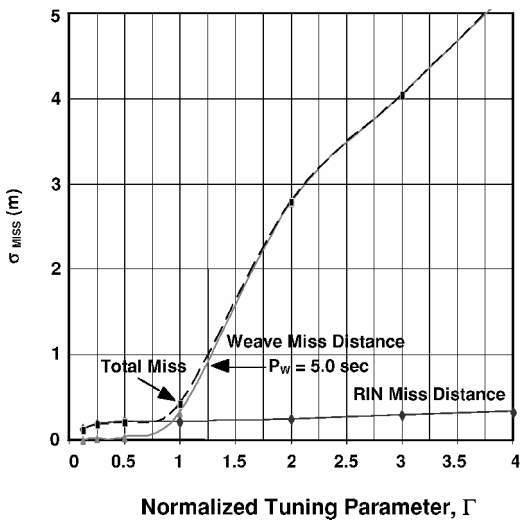

Fig. 8 Miss distance components and total for IR design example vs normalized tuning parameter Γ.

addressed in this paper, such as fin actuator rate or acceleration limits.

Figures 7 and 8 were all easy to generate (implemented here using spreadsheet analysis), given the normalized adjoint coefficients; they show the sensitivity of the design to the normalized parameter Γ.

V. Summary

This paper has presented the normalization technique for obtaining the steady-state adjoint miss distance variance sensitivities for the four-state OGS. These sensitivities have been developed and presented for the case of a single-pole autopilot, although the technique is applicable to other autopilot configurations. These sensitivities are a function of the newly developed normalized tuning parameter Γ, which is the range-independent component of Weiner filter time constant value at one autopilot time constant time to go, normalized to the autopilot time constant. Miss distance sensitivities for noise sources and target spiral maneuver are presented. Two performance analysis examples were presented, one for an rf seeker and one for an IR seeker, to illustrate the use of these equations. Tables and plots of the normalized adjoint miss distance coefficients can be generated for other values of Γ, T_1, T_2 and $T_{\min}$ by using the described procedures.

Curves in this paper for the optimal guidance system can be used by missile system designers to evaluate the variation of miss distance performance to the normalized tuning parameter Γ, for the various sources of miss distance, and the variation in the intercept parameters such as closing velocity and target weave period. The power of these equations is that the designer neither needs to use Monte Carlo simulations nor to solve the adjoint differential equations to visualize and evaluate the impact on miss distance performance of system design changes or intercept parameter variation. These equations are useful for designing robust missile guidance systems.

Appendix: Tables of Normalized Steady-State Miss Distance Coefficients

Table A1 Normalized steady-state miss distance variance coefficients[a]

	Γ								
Coefficient	0.0625	0.125	0.25	0.5	1	2	4	8	16
Uniformly distributed target maneuver $k_M(\Gamma)$	1.00E−4	2.00E−4	1.00E−3	1.19E−2	3.64E−1	2.38E+1	2.60E+3	3.64E+5	4.75E+7
Glint noise $k_0(\Gamma)$	1.01E+1	8.63E+0	6.27E+0	3.64E+0	1.81E+0	8.20E−1	3.50E−1	1.40E−1	6.00E−2
$k_1(\Gamma)$	6.90E−1	9.20E−1	1.12E+0	9.70E−1	6.90E−1	4.90E−1	3.80E−1	3.20E−1	2.90E−1
Range-independent angle noise $k_2(\Gamma)$	9.00E−2	1.80E−1	3.90E−1	5.50E−1	6.00E−1	7.80E−1	1.38E+0	3.05E+0	6.39E+0
$k_3(\Gamma)$	2.00E−2	6.00E−2	2.50E−1	6.70E−1	1.44E+0	4.52E+0	2.20E+1	1.26E+2	4.75E+2
Range-dependent semi-active angle noise $k_4(\Gamma)$	1.00E−2	3.00E−2	2.40E−1	1.34E+0	6.93E+0	5.92E+1	8.08E+2	1.08E+4	6.29E+4
$k_5(\Gamma)$	1.00E−2	2.00E−2	3.00E−1	3.87E+0	5.22E+1	1.24E+3	4.67E+4	1.29E+6	9.76E+6
Range-dependent active angle noise $k_6(\Gamma)$	5.30E−1	1.60E−1	4.80E−1	1.49E+1	5.49E+2	3.67E+4	3.71E+6	1.85E+8	1.60E+9

[a]IR case: single pole autopilot, $T_1 = 0$, $T_2 = \infty$, and $T_{\min} = 1$.

Table A2 M_{spiral} normalized steady-state miss distance standard deviation for target weave[a]

	Γ								
P_N	0.0625	0.125	0.25	0.5	1	2	4	8	16
0.1	1.10E+0	1.07E+0	1.03E+0	1.02E+0	1.01E+0	1.00E+0	1.82E+0	4.92E+1	4.96E−2
0.2	1.17E+0	1.17E+0	1.10E+0	1.05E+0	1.03E+0	1.01E+0	1.26E+0	2.46E+1	9.93E−2
0.5	1.00E+0	1.28E+0	1.29E+0	1.17E+0	1.09E+0	1.04E+0	1.07E+0	9.90E+0	2.48E−1
1	5.59E−1	8.27E−1	1.27E+0	1.25E+0	1.14E+0	1.07E+0	1.05E+0	5.03E+0	4.97E−1
2	1.70E−1	2.63E−1	6.20E−1	1.05E+0	1.08E+0	1.04E+0	1.02E+0	2.67E+0	9.95E−1
5	1.71E−2	2.65E−2	5.83E−2	2.91E−1	6.90E−1	8.48E−1	9.20E−1	1.40E+0	2.51E+0
10	2.43E−3	3.75E−3	8.09E−3	3.08E−2	2.84E−1	6.01E−1	7.80E−1	1.04E+0	5.18E+0
20	3.24E−4	4.96E−4	1.06E−3	3.76E−3	3.57E−2	3.11E−1	5.91E−1	8.36E−1	1.14E+1
50	2.17E−5	3.30E−5	6.95E−5	2.43E−4	1.66E−3	3.33E−2	2.86E−1	5.88E−1	4.40E+1
100	2.77E−6	4.20E−6	8.79E−6	3.05E−5	2.05E−4	2.63E−3	8.00E−2	3.66E−1	1.29E+2

[a]IR case: single pole autopilot, $T_1 = 0$, $T_2 = \infty$, and $T_{\min} = 1$.

Table A3 Normalized steady-state miss distance variance coefficients[a]

	Γ								
Coefficient	0.0625	0.125	0.25	0.5	1	2	4	8	16
$k_M(\Gamma)$	3.00E−4	1.60E−3	1.62E−2	2.56E−1	5.92E+0	1.98E+2	9.94E+3	7.56E+5	6.83E+7
$k_0(\Gamma)$	1.11E+1	7.74E+0	4.34E+0	2.17E+0	1.05E+0	5.00E−1	2.30E−1	1.00E−1	4.00E−2
$k_1(\Gamma)$	2.07E+0	2.41E+0	1.97E+0	1.38E+0	9.80E−1	7.40E−1	5.60E−1	4.40E−1	3.60E−1
$k_2(\Gamma)$	6.00E−1	1.27E+0	1.66E+0	1.80E+0	2.11E+0	2.70E+0	3.70E+0	5.71E+0	8.95E+0
$k_3(\Gamma)$	2.40E−1	1.00E+0	2.27E+0	4.34E+0	9.60E+0	2.45E+1	7.29E+1	2.51E+2	6.74E+2
$k_4(\Gamma)$	1.20E−1	9.90E−1	4.14E+0	1.51E+1	6.82E+1	3.88E+2	2.85E+3	2.17E+4	8.90E+4
$k_5(\Gamma)$	8.00E−2	1.17E+0	9.24E+0	6.67E+1	6.53E+2	8.94E+3	1.69E+5	2.57E+6	1.38E+7
$k_6(\Gamma)$	5.80E−1	1.70E+0	2.42E+1	3.58E+2	7.97E+3	2.77E+5	1.35E+7	3.68E+8	2.27E+9

[a]RF case: single pole autopilot, $T_1 = 4$, $T_2 = \infty$, and $T_{\min} = 1$.

Table A4 M_{spiral} normalized steady-state miss distance standard deviation for target weave[a]

	Γ								
P_N	0.0625	0.125	0.25	0.5	1	2	4	8	16
0.1	1.03E+0	1.02E+0	1.01E+0	1.00E+0	9.99E−1	9.99E−1	3.36E+0	7.45E+1	4.96E−2
0.2	1.13E+0	1.06E+0	1.03E+0	1.01E+0	1.01E+0	1.00E+0	1.89E+0	3.73E+1	9.93E−2
0.5	1.85E+0	1.38E+0	1.17E+0	1.08E+0	1.04E+0	1.02E+0	1.19E+0	1.49E+1	2.48E−1
1	1.23E+0	1.97E+0	1.48E+0	1.22E+0	1.10E+0	1.05E+0	1.07E+0	7.52E+0	4.97E−1
2	3.20E−1	8.43E−1	1.67E+0	1.38E+0	1.18E+0	1.09E+0	1.05E+0	3.87E+0	9.95E−1
5	2.95E−2	7.28E−2	2.80E−1	1.03E+0	1.19E+0	1.10E+0	1.05E+0	1.84E+0	2.51E+0
10	4.08E−3	9.76E−3	3.63E−2	1.98E−1	8.20E−1	1.02E+0	1.02E+0	1.30E+0	5.18E+0
20	5.34E−4	1.26E−3	4.61E−3	2.41E−2	1.83E−1	6.93E−1	8.94E−1	1.06E+0	1.14E+1
50	3.52E−5	8.18E−5	2.97E−4	1.54E−3	1.01E−2	1.08E−1	5.02E−1	7.89E−1	4.40E+1
100	4.46E−6	1.03E−5	3.72E−5	1.93E−4	1.26E−3	1.01E−2	1.56E−1	5.07E−1	1.29E+2

[a]RF case: single pole autopilot, $T_1 = 4$, $T_2 = \infty$, and $T_{min} = 1$.

Acknowledgment

This work is sponsored by the Electronic Systems Command under U.S. Air Force Contract F19628-00-C-0002. Opinions, interpretations, recommendations, and conclusions are those of the author and are not necessarily endorsed by the United States Government.

References

[1]Nesline, F. W., and Zarchan, P., "Miss Distance Dynamics in Homing Missiles," AIAA Paper 84-1844, Aug. 1984.

[2]Zarchan, P., "Complete Statistical Analysis of Nonlinear Missile Guidance Systems: SLAM," *Journal of Guidance and Control*, Vol. 2, No. 1, 1979, pp. 71–78.

[3]Howe, R. M., *Systems Engineering Handbook*, edited by R. E. Machol, McGraw–Hill, New York, 1965, Chap. 19.

[4]Laning, J. H., and Battin, R. H., *Random Processes in Automatic Control*, McGraw–Hill, New York, 1956, Chap. 6 and Appendix F.

[5]Peterson, E. L., *Statistical Analysis and Optimization of Systems*, Wiley, New York, 1961, Chaps. 4, 6.

[6]"The Method of Adjoint System and Its Application to Guided Missile Noise Studies," EASAMS, National Technical Information Service Rept. PB186191, Camberley, England, U.K., July 1969.

[7]Fitzgerald, R. J., and Zarchan, P., "Shaping Filters for Randomly Initiated Target Maneuvers," *Proceedings of the AIAA Guidance and Control Conference*, AIAA, New York, 1978, pp. 424–430.

[8]Zarchan, P., "Representation of Realistic Evasive Maneuvers by the Use of Shaping Filters," *Journal of Guidance and Control*, Vol. 2, No. 4, 1979, pp. 290–295.

[9]Alpert, J., "Miss Distance Analysis for Command Guided Missiles," *Journal of Guidance, Control, and Dynamics*, Vol. 11, No. 6, 1988, pp. 481–487.

[10]Zarchan, P., "Proportional Navigation and Weaving Targets," *Journal of Guidance, Control, and Dynamics*, Vol. 18, No. 5, 1995, pp. 969–974.

[11]Nesline, F. W., and Zarchan, P., "A New Look at Classical Versus Modern Homing Missile Guidance," *Journal of Guidance and Control*, Vol. 4, No. 1, 1981, pp. 78–85.

[12]Nesline, F. W., and Nesline, M. L., "An Analysis of Optimal Command Guidance vs. Optimal Semi-Active Homing Missile Guidance," *Proceedings of the 1986 American Control Conference*, Vol. 2, Inst. of Electrical and Electronics Engineers, New York, 1986, pp. 1103–1111.